

# Hydrodynamic optimization of pump-turbine runner

Denis Chirkov<sup>1\*</sup>, Vladimir Skorospelov<sup>2</sup>, Polina Turuk<sup>2</sup>, Valeriy Rigin<sup>3</sup>, and Alexander Ustimenko<sup>3</sup>

<sup>1</sup>Kutateladze Institute of Thermophysics SB RAS, 630090 Lavrentiev avenue 1, Novosibirsk, Russia

<sup>2</sup>Sobolev Institute of Mathematics SB RAS, 630090 Koptyug avenue 4, Novosibirsk, Russia

<sup>3</sup>JSC Power Machines, 195009 Vatutina st. 3 lit.A, Saint-Petersburg, Russia

**Abstract.** The paper suggests the approach to automatic CFD-based optimization of the pump-turbine runner. An in-house 3D flow solver CADRUN is used for the solution of steady-state RANS equations and evaluation of objective functions in representative operating points of turbine and pump operating regimes. Both efficiency and cavitation characteristics are taken into account. Two approaches have been considered, resulting in 4- and 3-objective shape optimization problems. These problems were solved using multi-objective genetic algorithm. It was shown that the obtained optimized runners feature increased efficiency both in turbine and pump mode with cavitation performance, similar to that of the initial runner.

## 1 Introduction

The paper is devoted optimal design of runner for pump-turbine, the heart of the pumped-storage power plants (PSPP). Pump-turbines, Fig.1, alternately operate in two operating modes: turbine mode and pump mode. In turbine mode the water flow, going down through the turbine from upper reservoir, rotates the runner. The generator transforms the energy of runner rotation to electricity. In case of excess of energy in electrical grid the power station switches to pump mode, now generator serving as electric motor, rotates the runner, which in its turn pumps the water from lower reservoir back to upper reservoir, thus storing the energy for future use.

Besides two operating modes, having different flow phenomena, operation of pump-turbines is associated with additional features. These are the increased dynamic loads on the runner blades and guide vanes, due to the narrow gap between them, and strong influence of cavitation on the efficiency both in turbine and pump modes. Thus the flow passage of the pump-turbine should satisfy multiple contradictive criteria, which complicates the problem of flow passage design.

Modern CFD tools allow accurate enough computation of efficiency and cavitation characteristics of pump-turbines in a given operating regime. The present paper suggests an approach to automatic shape optimization of the pump-turbine runner based on 3D steady flow simulation and evolutionary algorithm for the solution of multi-objective optimization problem.

## 2 CFD simulations

### 2.1 CFD solver and boundary conditions

During the optimization 3D flow field computations were carried out using an in-house CFD solver CADRUN, briefly described in [1, 2]. Artificial compressibility finite-volume numerical method is used for the solution of RANS equations. Either k- $\epsilon$  or SST model is used for turbulence. Third order accurate MUSCL scheme is used for evaluation of inviscid fluxes, while 2nd order central difference scheme is used for evaluation of viscous fluxes. The code is explained in detail in [3].

Periodic stage approach was employed to ensure fast computation of the flow-field. Fig. 2 shows the block-structured mesh for the wicket channel (between the neighbouring guide vanes), the rotating runner channel (between the two blades), and upper part of the draft tube. Averaging of all flow parameters was employed at mixing plane interfaces between wicket gate and runner, and between runner and draft tube.

In turbine mode constant flow angle, and constant total flow energy  $E_{1A}$  are specified in the inlet of the wicket gate channel (Fig.1, section 1A), while constant flow energy  $E_2$  is specified in the outlet section of the draft tube (section 2). Note, that  $E_{1A} - E_2 = H - h_{SP}$ , where  $H$  is a prescribed turbine head,  $h_{SP}$  – is the preliminary estimated or computed energy loss in the spiral casing, which is located upstream the wicket gate, Fig. 1. With these boundary conditions the value of discharge  $Q$  is not known a priori, but obtained in the process of solution. Finally, the pump-turbine efficiency in turbine mode  $\eta_T$  is evaluated using the formula

\* Corresponding author: [chirkov.itp@gmail.com](mailto:chirkov.itp@gmail.com)

$$\eta_T = \frac{M\omega}{\rho gQH} \eta_{mech} \eta_{vol}, \quad (1)$$

where  $M$  is the computed runner torque,  $\omega$  is the rotation frequency,  $Q$  is the computed discharge,  $H$  is the fixed turbine head.  $\eta_{mech}$  and  $\eta_{vol}$  are the mechanical and volume efficiencies, accounting for the disc friction and leakage flow, respectively. They are estimated via engineering formulas.

In pump mode the runner rotates in the opposite direction and pumps the fluid to upper reservoir. The inlet and outlet cross sections change their roles. Section 2 in the draft tube becomes the inlet, here the constant uniform velocity, corresponding to the given discharge  $Q$  is fixed. In the outlet from the wicket gate (section 1A) the uniform pressure distribution is specified. With this statement of boundary conditions the value of total head  $H$  is not known a priori, and is found after CFD simulation is converged. Note, that spiral casing loss  $h_{SP}$  should be subtracted from the energy difference  $E_{1A} - E_2$  between sections 1A and 2 to obtain turbine head:

$$H = E_1 - E_2 - h_{SP}. \quad (2)$$

Ideally,  $h_{SP}$  should also be computed using 3D CFD in the complete spiral casing. However, this computation is time consuming, therefore simplified approaches are often used within optimization loop. One of them is to assume that  $h_{SP}$  is independent of runner shape. In this case  $h_{SP}$  is computed once for the initial runner and then used for evaluation of total head for other runner modifications. Finally, pump-turbine efficiency  $\eta_P$  in pump mode is evaluated using the formula

$$\eta_P = \frac{QH}{M\omega} \eta_{mech} \quad (3)$$

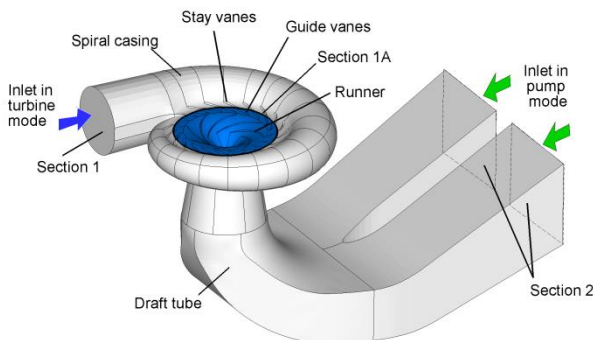


**Fig. 1.** Pump-turbine flow passage.

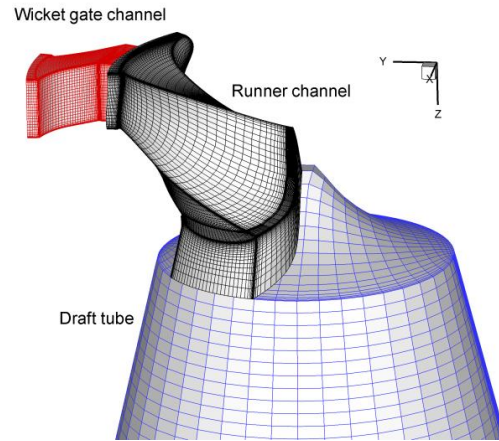
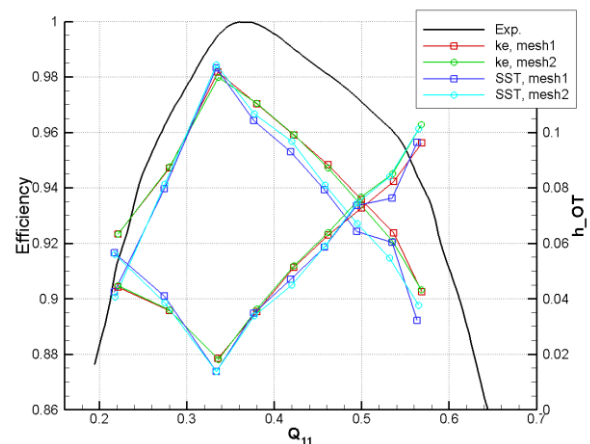


**Fig. 2.** Computational domain and block-structured mesh in WG, runner and draft tube of pump-turbine.

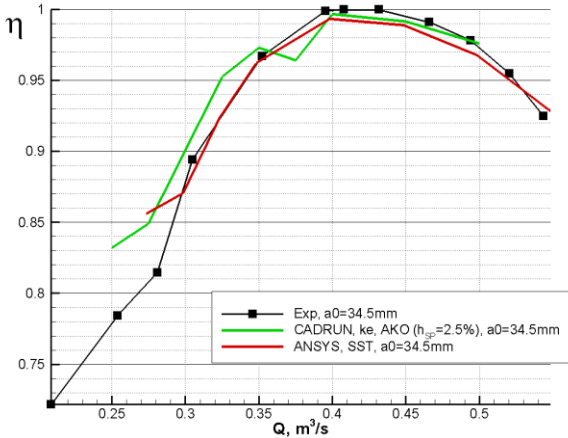
## 2.2 Efficiency prediction

Fig. 3 shows normalized efficiency of the initial pump-turbine in turbine mode. Shown are the experimental data and computations using CADRUN with ke and SST turbulence models. Mesh1 is the basic mesh, while mesh2 is 1.5 times refined in all special dimensions. Both turbulence models and meshes give similar result: in computations the efficiency is 2-3% lower, than in the experiment. It is probably due to the increased draft tube loss, which dependence on the discharge looks like a reflection of efficiency dependence on discharge, Fig. 3. This issue needs to be investigated further.

Fig. 4 compares pump mode efficiency as function of turbine discharge, obtained via computations in ANSYS CFX and CADRUN to experimental efficiency. Good agreement is observed in a wide range of operating points.



**Fig. 3.** Normalized efficiency hill chart and energy losses in the draft tube. Initial runner, turbine mode.



**Fig. 4.** Normalized efficiency hill chart. Initial runner, pump mode. Computations in ANSYS CFX and CADRUN vs experimental data.

### 2.3 Cavitation analysis

One of the most important criteria of pump turbine quality is its cavitation performance, which is the dependence of its efficiency on the cavitation coefficient, which is defined according to IEC 60193 standard

$$\sigma_{nD} = \frac{NPSE}{n^2 D^2},$$

where NPSE is the net positive suction energy,  $n$  is the runner rotation frequency,  $D$  is the runner diameter.

For numerical prediction of cavitation curve, series of cavitation CFD simulations have to be performed for different values of  $\sigma_{nD}$ . In this paper Zwart-Gerber-Belamry model [4] is used to account for cavitation. Fig. 5 shows the predicted cavitation curve for the initial runner. Good agreement of computation using CADRUN to both ANSYS prediction and experimental data is seen.

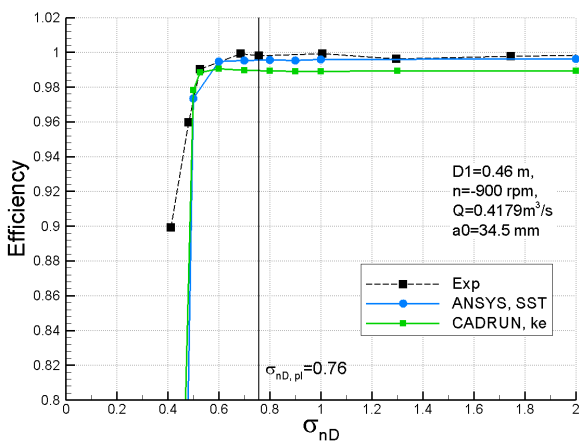


**Fig. 5.** Initial runner. Cavitation curve in pump mode. Comparison of experimental data and computations using ANSYS CFX and CADRUN.

## 3 Runner optimization approach

### 3.1 Runner parameterization

The shape of the runner is parameterized by 24 parameters, describing the blade chamber surface, and meridian projections of hub and shroud [1]. In the present study the blade thickness distribution is assumed constant, but can easily be turned on, using the approach, described in [2].

### 3.2 Optimization algorithm

For the solution of the multi-objective optimization problem a genetic algorithm MOGA is used [5]. In case of 24 free geometric parameters and 3-4 objective functions it requires consideration of several thousands of runner variants. Within optimization loop CFD analysis is performed for each runner variant using the numerical setup, described in section 2.

## 4 Results

The flow passage of the pump turbine should ensure a number of generally contradictive criteria, such as high efficiency both in turbine mode and in pump mode, minimal cavitation phenomena in a wide range of discharges, required level of head in pump mode, etc. Pursuing all of them in a single optimization run would lead to high number of objective functions. Increasing the number of objective functions, in its turn, dramatically increases the computational efforts (increased population size, increased number of generations in MOGA algorithm), required for obtaining converged Pareto front. One of the compromise approaches is to consider only the most important objectives. The other can be formulated as constraints or even ignored within optimization loop. The latter are to be checked after the optimization. In the present paper two multi-objective problem statements were considered.

In the first statement (Opt1) 4 objective functions were simultaneously activated:

- maximization of efficiency  $\eta_1$  in best efficiency point (BEP) in turbine mode;
- maximization of efficiency  $\eta_2$  in BEP in pump mode;
- minimization of  $A_{cav}$  in BEP in turbine mode;
- minimization of  $A_{cav}$  in BEP in pump mode.

In this statement all the CFD computations were performed in frames of single phase incompressible RANS equations. Here cavitation performance in both operating points was estimated using the value of  $A_{cav}$ , the relative area of zone on the suction side of the runner blade, where the pressure is lower, than the vapor pressure. Additionally in Opt1 the constraints on the turbine head in pump mode were set.

In the second optimization statement (Opt2) the efficiency in BEP in pump mode was evaluated using two-phase cavitation model. Thus, cavitation performance in this regime was evaluated directly, without the need for  $A_{cav}$ . This approach allowed to reduce the number of objectives to 3 objective functions:

- maximization of efficiency  $\eta_1$  in best efficiency point (BEP) in turbine mode;
- maximization of efficiency  $\eta_2$  in BEP in pump mode (evaluated with two-phase cavitation model);
- minimization of  $A_{cav}$  in BEP in turbine mode.

As in Opt1 the constraints on the turbine head in pump mode were set in Opt2.

In both optimization runs several dozens of generations of MOGA have been computed with 144 individuals (runner variants in each). As an example, Fig. 6 shows the obtained Pareto front for optimization Opt2. The values of efficiency in turbine and pump modes were normalized by the computed efficiencies of the initial runner. It can be seen, that optimization was able to substantially increase efficiency of the pump-turbine both in turbine and pump mode.

From the computed Pareto fronts for optimizations Opt1 and Opt2 several perspective variants have been selected. Fig. 7 compares the shapes of the initial runner to optimized runner VR1, selected from Opt1, and optimized runner VR2, selected from Opt2. It can be seen that the shapes of the leading edge differ significantly.

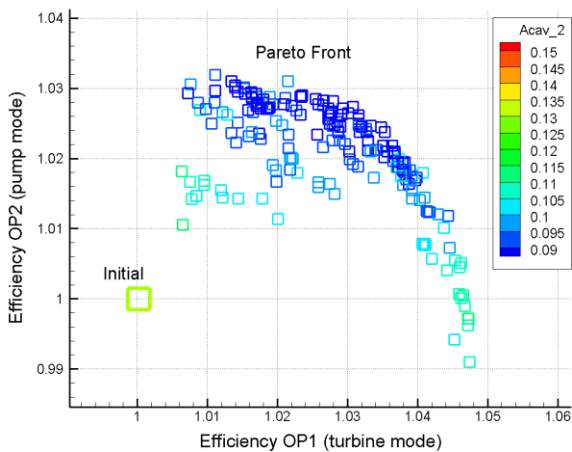


**Fig. 6.** Pareto front for optimization Opt2.

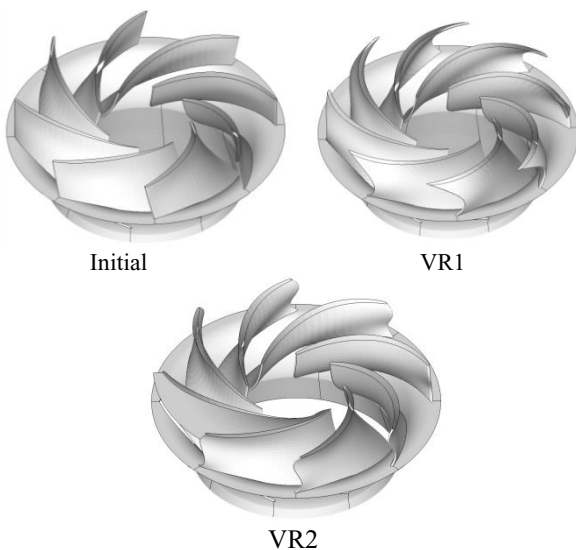


**Fig. 7.** Comparison of runner shapes.

In order to check cavitation performance, cavitation curves have been computed for VR1 and VR2. Fig. 8

compares the computed cavitation curve for VR1 to that of the initial runner in pump mode. It can be seen that although the value of relative cavitation zone  $A_{cav}$  has been reduced for VR1, the cavitation curve for this variant is worse than that of the initial one. This fact indicates, that indirect estimation of cavitation characteristics through the value of  $A_{cav}$  is not always appropriate in pump mode. Fig. 9 shows the predicted cavitation curve for VR2. It turned to be superior to VR1, since the drop of efficiency is observed at lower  $\sigma_{nD}$  value,  $\sigma_{nD} = 0.6$ , which is close to the critical cavitation coefficient of the initial runner.

Fig. 10 compares the distributions of the vapor phase in the inter-blade channel of the runner VR1 for different  $\sigma_{nD}$ . One can see the incipience of cavitation on the suction side near the leading edge. Note that although no efficiency drop is observed in Fig. 9 for  $\sigma_{nD} = 0.6$  and 0.8, these operating points are not cavitation free. Fig. 10 shows that small area of cavitation persist even at  $\sigma_{nD} = 2$ . The same situation is observed for the initial runner and for VR2. Further improvements of the optimization setup have to be performed in order to completely remove runner cavitation for  $\sigma_{nD} > 0.6$ .

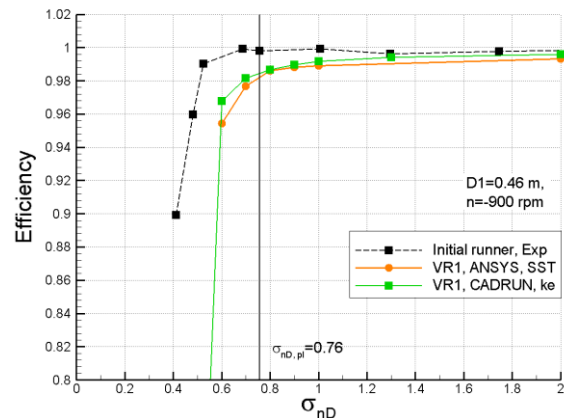


**Fig. 8.** Runner VR1. Cavitation curve in pump mode. Computations using ANSYS CFX and CADRUN, compared to experimental data of the initial runner.

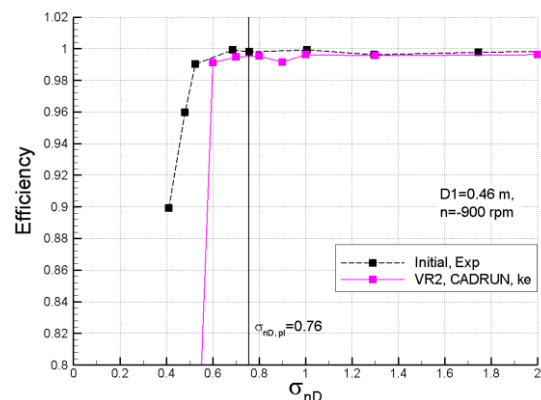


**Fig. 9.** Runner VR2. Cavitation curve in pump mode. Comparison of computations using CADRUN to experimental data of the initial runner.

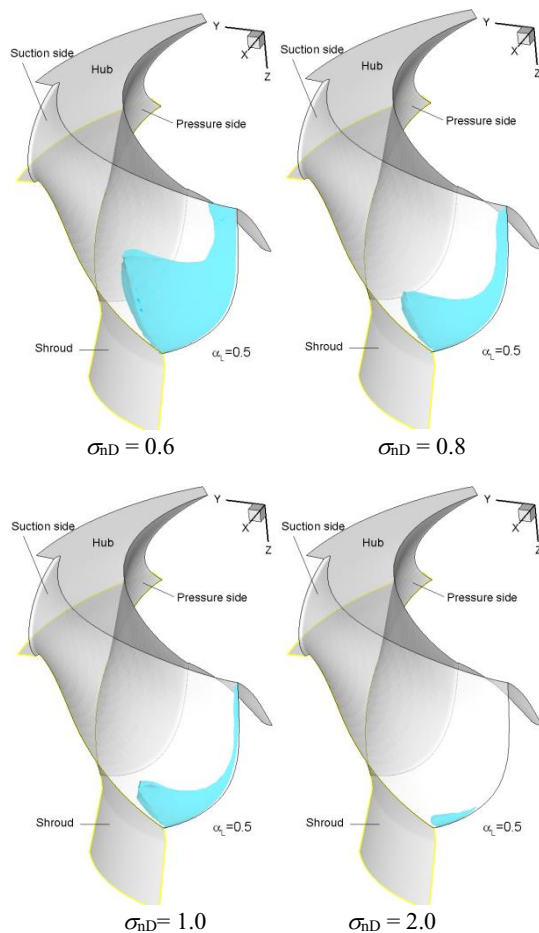


**Fig. 10.** Runner VR1. Vapor cavity in the runner channel (iso-surface  $\alpha_L = 0.5$ ).

## 5 Conclusion

A multi-objective optimization of the pump-turbine runner, based on steady state CFD simulations of the flow-field is performed. Both efficiency and cavitation characteristics in representative turbine mode and pump mode operating points are taken into account. Two approaches have been considered, resulting in 4- and 3-objective shape optimization problems. Both approaches offer a number of runner variants, suggesting higher efficiency. In order to check the performance of the optimized runners in wide range of operating points, efficiency hill charts and cavitation curves have been computed. It was shown that the obtained optimized runners feature increased efficiency both in turbine and pump mode with cavitation performance, similar to that of the initial runner. However, optimization was not able to completely remove cavitation for the desired range of  $\sigma_{nD}$  values. Future investigations have to be carried out to resolve this problem. Another issue is the increase of accuracy of efficiency prediction in turbine mode, the lack of which was observed in computations of the initial runner. The other directions for future research are the unsteady analysis of rotor-stator interaction and stress analysis of the optimized runners.

## References

1. A.E. Lyutov, D.V. Chirkov, V.A. Skorospelov, P.A. Turuk, S.G. Cherny, *ASME J. of Fluids Eng.* **137**, 111302 (2015)
2. D.V. Chirkov, A.S. Ankudinova, A.E. Kryukov, S.G. Cherny, V.A. Skorospelov, *Structural and Multidisciplinary Optimization* **58**(2), 627 (2018)
3. S.G. Cherny, D.V. Chirkov, V.N. Lapin, et al. *Chislennoe modelirovanie techeniy v turbomashinah*, Ed.: Novosibirsk, Nauka, 202 p. (2006, in Russian)
4. P.J. Zwart, A.G. Gerber, T.A. Belamri *Two-phase flow model for predicting cavitation dynamics*. In Proc. of International Conference on Multiphase Flow, Paper 152 (Yokohama, Japan, 2004)
5. D.V. Bannikov, S.G. Cherny, D.V. Chirkov, V.A. Skorospelov, P.A. Turuk, *Vichislitel'nie tekhnologii* **14** (2) 32 (2009, in Russian)